



Normal and High-Strength Lightweight Self-Compacting Concrete Incorporating Perlite, Scoria, and Polystyrene Aggregates at Elevated Temperatures

Farhad Aslani, M.ASCE¹; and Guowei Ma²

Abstract: Lightweight self-compacting concrete (LWSCC) is an advanced concrete that combines the advantages of both lightweight concrete (LWC) and self-compacting concrete (SCC). This concrete provides an excellent solution to decreasing the self-weight of a structure while making pouring easier and removing the construction challenges and complications. This study examined the impact of elevated temperatures on normal-strength lightweight self-compacting concrete (NSLWSCC) and high-strength lightweight self-compacting concrete (HSLWSCC) through its residual properties vis-à-vis compressive and tensile strengths, modulus of elasticity, mass loss, and spalling intensity. LWSCCs were designed using lightweight aggregate (LWA), which replaced coarse and fine aggregates at certain percentages. Three types of LWA used in this study are scoria, perlite, and polystyrene. Mixes consisted of six NSLWSCCs (50% and 100% scoria, 50% and 100% perlite, 20% and 30% polystyrene) and two HSLWSCCs (50% scoria). The residual properties were measured by heating 100 × 200 mm cylinder specimens to 100°C, 300°C, 600°C, and 900°C. The result shows that the NSLWSCCs tend to achieve maximum strength at 100°C and then gradually decrease as the temperature increases. But in the case of HSLWSCCs, maximum strength was achieved at 300°C. Minor spalling with bubbles, holes, and cracking was observed at only 900°C in the NSLWSCC, while a major explosion occurred at 300°C in the HSLWSCC. The overall result indicates that the magnitude of loss of strength, mass loss, and intensity of spalling is proportional to temperature after a certain point. This study shows how the strength and thermal stability of LWSCC made from scoria, perlite, and polystyrene changes after exposure to high temperatures. DOI: [10.1061/\(ASCE\)MT.1943-5533.0002538](https://doi.org/10.1061/(ASCE)MT.1943-5533.0002538). © 2018 American Society of Civil Engineers.

Author keywords: Self-compacting concrete (SCC); Lightweight concrete (LWC); Lightweight self-compacting concrete (LWSCC); High temperatures; Fire; Perlite, scoria, and polystyrene aggregates.

Introduction

Self-compacting concrete (SCC), also known as self-consolidating concrete, is a highly flowable and nonsegregating concrete that can fill and spread in formwork under its own weight without any mechanical vibration. The development of SCC took place in Prof. Okumara's laboratory in Japan in 1986 as a solution against the drawback of conventional concrete in densely placed steel reinforcement and to overcome the declining number of qualified concrete workers (Okamura et al. 2000; De Schutter et al. 2008; Aslani and Kelin 2018). The use of SCC has reduced direct labor costs and construction period durations. Furthermore, SCC has substantial technical advantages on concreting high and thin walls containing dense reinforcement as well as posttensioning ducts (De Schutter et al. 2008).

The method of SCC design differs from that of ordinary concrete with respect to two opposite properties, flowability and

segregation resistance (Choi et al. 2006; Aslani 2013a, 2014, 2015b, a; Aslani et al. 2018a, b; Law Yim Wan et al. 2018). To optimize the workability of SCC, a low yield stress and a moderate viscosity are required to ensure that aggregates do not segregate during flow (Andiç-Çakir et al. 2009; Aslani et al. 2017, 2018a, b; Aslani and Bastami 2014; Aslani and Samali 2014b). The segregation resistance of SCC is due to the high viscosity and the countereffect of fine particles in admixtures to prevent aggregates from floating or sinking (Bogas et al. 2012; Aslani and Maia 2013; Aslani and Natoori 2013; Maia and Aslani 2016; Aslani et al. 2018a, b). Although there are many benefits of SCC in comparison to normal concrete, the high costs of the materials necessary to produce SCC and the resulting high unit weight have served as limiting factors of its application in the construction industry (Gesoglu et al. 2014).

Lightweight self-compacting concrete (LWSCC) aims to combine the benefits of both lightweight concrete (LWC) and SCC, which can offer engineers greater freedom when it comes to designing efficient concrete structures with respect to project costs and time. The addition of lightweight aggregates (LWAs) in concrete to produce LWC can result in a higher strength-to-weight ratio, enhance thermal properties and fire resistance, and lead to a decrease in dead loads (Kivrak et al. 2006; Abdelaziz 2010). Decreases in dead loads are beneficial in the construction industry because they can result in cost savings stemming from the reduction of the size of structural elements and possibly the amount of steel reinforcement required (Abdelaziz 2010).

The large difference in the densities of LWAs and binders increases the possibility of segregation (Bogas et al. 2012; Aslani et al. 2018a, b). The main problems associated with porous LWAs

¹Senior Lecturer, School of Civil, Environmental, and Mining Engineering, Univ. of Western Australia, Perth, WA 6009, Australia; Adjunct Associate Professor, School of Engineering, Edith Cowan Univ., Perth, WA 6027, Australia (corresponding author). Email: farhad.aslani@uwa.edu.au

²Professor, School of Civil, Environmental, and Mining Engineering, Univ. of Western Australia, Perth, WA 6009, Australia.

Note. This manuscript was submitted on January 25, 2018; approved on June 15, 2018; published online on October 4, 2018. Discussion period open until March 4, 2019; separate discussions must be submitted for individual papers. This paper is part of the *Journal of Materials in Civil Engineering*, © ASCE, ISSN 0899-1561.

are their high absorption of water during the mixing process and the tendency of lighter aggregates to float, increasing the risk of segregation (Ranjbar and Mousavi 2015). This segregation can be controlled by the addition of sufficient viscosity-modifying admixtures (VMAs) or increasing the binder content, thereby ensuring that there is sufficient viscosity to suspend aggregates within the binder without significantly affecting its flow properties (Andiç Çakir et al. 2009).

Hassan et al. (2015) showed that as the percentage of LWAs increases, the density of the mixture is reduced and the slump flow diameter decreases. Similarly, findings by Abouhussien et al. (2015) showed that increasing the ratio of LWA to sand caused an increase in V-funnel times, indicating a negative impact on its workability. However, Gesoglu et al. (2015) showed that improving the quality and obtaining a more spherical shape of aggregates resulted in less internal friction and blocking of the mixture, thereby improving the flowability of SCC.

Abdelaziz (2010) investigated the increase of admixture [superplasticizer (SP) and VMA] dosage on slump flow. The slump flow of LWSCC increased with increasing admixture dosage until a certain dosage limit was reached, and thereafter the slump flow decreased. This dosage limit is associated with the chemical admixture's ability to reduce attractive forces between oppositely charged particles and increase interparticle repulsive forces. Hence, increasing the dosage led to increased viscosity and the amount of negatively charged particles, which in turn decreased the slump flow diameter.

The introduction of LWAs in SCC has a negative impact on the compressive strength of LWSCC (Topcu and Uygunoglu 2010). However, increasing the quality of the LWAs as indicated by lower absorption rates results in less reduction in compressive strength (Kim et al. 2010). Compressive strength is related to the absorption and particle shape of LWAs that affect the interaction between the aggregates and the cement paste (Yehia et al. 2014). LWSCC has a lower splitting tensile strength compared to normal concrete; this is because of the splitting tension that occurs through the LWAs rather than the cement paste due to its naturally weaker strength path (Gesoglu et al. 2014). Concrete mixtures tend to develop a higher splitting tensile strength early on than normal concrete; however, in later stages, this strength is limited by the strength limitations of LWAs, where splitting tension occurs (Her-Yung 2009).

Moreover, in the last few years, a good deal of research has been done on the fire behavior of high-performance concrete (Husem 2006; Ario 2007; Koksal et al. 2012). It is well known that exposure to fire or elevated temperatures from any extreme heat source has adverse effects on concrete's mechanical and physical properties (Gai-Fei and Zhi-Shan 2008; Bingol and Gul 2004; Poon et al. 2004; Koksal et al. 2012). Thus, although concrete generally provides adequate fire resistance for most applications, its strength and durability properties are significantly affected when subjected to elevated temperatures due to chemical and physical changes. For example, in terms of loss in compressive strength, the critical temperature range is between 600°C and 800°C. The durability and mechanical properties of concrete subjected to elevated temperatures have been the subject of study of many researchers who have investigated various fire-resistant materials (Koksal et al. 2012; Khaliq and Kodur 2011; Wenzhong et al. 2012; Gencel 2011).

While numerous studies have been conducted on the thermal characteristics of NWSCC and many have been performed investigating the characteristics of LWSCC (Kim et al. 2010; Wu et al. 2009; Lo et al. 2007), few studies have examined the effects of prolonged exposure to high temperatures on the physical and mechanical properties of LWSCC in comparison with NWSCC (Wu et al. 2013; Bozkurt 2014; Fares et al. 2015).

Research Significance

The research presented here will explore the ability of materials locally available in Australia to produce normal-strength LWSCC (NSLWSCC) and high-strength LWSCC (HSLWSCC), including LWAs, fillers, SP, sand, and others. This will help in standardizing local materials and getting an idea of the strength it can generate and its durability against fire. Consequently, it may also promote the economic and sustainable use of LWSCC in Australia.

Table 1. Properties of cement

Properties	Values
	Chemical
CaO	63.40%
SiO ₂	20.10%
Al ₂ O ₃	4.60%
Fe ₂ O ₃	2.80%
SO ₃	2.70%
MgO	1.30%
Na ₂ O	0.60%
Total chloride	0.02%
	Physical
Specific gravity	3.0–3.2 t/m ³
Fineness index	390 m ² /kg
Normal consistency	27%
Setting time initial	120 min
Setting time final	210 min
Soundness	2 mm
Loss on ignition	3.80%
Residue 45 µm sieve	4.70%
	Mechanical
Mortar compressive strength	
f'_c 3 days	38.6 MPa
f'_c 7 days	48.4 MPa
f'_c 28 days	58.5 MPa
Shrinkage at 28 days	640 µ strain

Table 2. Properties of fly ash

Properties	Values
	Chemical
CaO	3.30%
SiO ₂	50.40%
Al ₂ O ₃	31.50%
Fe ₂ O ₃	10.40%
SO ₃	0.10%
MgO	1.10%
Na ₂ O	0.30%
K ₂ O	0.50%
SrO	<0.1%
TiO ₂	1.90%
P ₂ O ₅	0.50%
Mn ₂ O ₃	0.20%
Total alkali	0.60%
	Physical
Relative density	2.29
Moisture	<0.1%
Loss on ignition	1.10%
Sulfuric anhydride	0.10%
Chloride ion	0.00%
Chemical composition	92.30%
Relative water requirement	93%
Strength index	102%

Table 3. Properties of ground granulated blast furnace slag

Properties	Values
	Chemical
S	0.40%
SO ₃	2.40%
MgO	5.70%
Al ₂ O ₃	12.60%
FeO	0.80%
MnO	0.10%
Cl	0.01%
Insoluble residue content	0.20%
	Physical
Specific gravity	3.0–3.2
Relative water requirement	103%
Relative strength	100%
Temperature rise	18.8°C
Fineness (passing 45 µm)	98%

Table 4. Properties of silica fume

Properties	Values
	Chemical
Silicon as SiO ₂	98%
Sodium as Na ₂ O	0.33%
Potassium as K ₂ O	0.17%
Available alkali	0.40%
Chloride as Cl ⁻	0.15%
Sulphuric anhydride	0.83%
Sulphate as SO ₃	0.90%
	Physical
Bulk density	625 kg/m ³
Relative density	2.21
Pozzolanic activity at 7 days	111%
Control mix strength	31.3 MPa
Moisture content	1.10%
Loss of ignition	2.40%

Table 5. Natural crushed 10 mm aggregate distribution

Sieve size	Percentage passing
13.2 mm	100
9.5 mm	87
6.7 mm	20
4.75 mm	7
2.35 mm	4
1.18 mm	3
600 µm	2
300 µm	2
150 µm	2
75 µm	2

This study will also provide information on the mix design of NSLWSCC and HSLWSCC made from scoria, perlite, and polystyrene along with the residual mechanical properties (compressive strength and tensile strength) under various temperature conditions. The information in the form of test results and data can serve as a guide for structural/design engineers using LWSCC. Additionally, it can be a guideline for the safe use of structures built from LWSCC. Thus, it can form the basis for the development of Australian standards for the fire resistance of LWSCC for structural purposes and serve as safety guidelines.

Table 6. Physical properties of natural crushed 10 mm aggregates

Physical property	Value (%)
Moisture content	0.5
Flakiness index	24.0

Table 7. Natural crushed < 4 mm aggregate distribution

Sieve size	Percentage passing
4.75 mm	100
2.36 mm	80
1.18 mm	55
600 µm	39
300 µm	27
150 µm	18
75 µm	13

Table 8. Physical properties of natural crushed < 4 mm aggregates

Physical property	Value
Apparent particle density	2.76 t/m ³
Particle density dry	2.65 t/m ³
Particle density SSD	2.69 t/m ³
Water absorption	1.40%
Moisture content	2.50%

Note: SSD = saturated surface dry.

Table 9. Chemical properties of natural fine sand

Chemical property	Value (%)
SiO ₂	99.86
Fe ₂ O ₃	0.01
Al ₂ O ₃	0.02
CaO	0.00
MgO	0.00
Na ₂ O	0.00
K ₂ O	0.00
TiO ₂	0.03
MnO	<0.001

Table 10. Natural fine sand aggregate distribution

Sieve size (µm)	Percentage retained
850	0
600	0.30
425	11.90
300	40.80
212	31.60
150	12.60
106	2.30
75	0.20

Table 11. Physical properties of natural fine sand

Physical property	Value (%)
Loss on ignition	0.01
Water content (at 105°C)	<0.001
AFS number	47.50

Note: AFS = American Foundry Society.

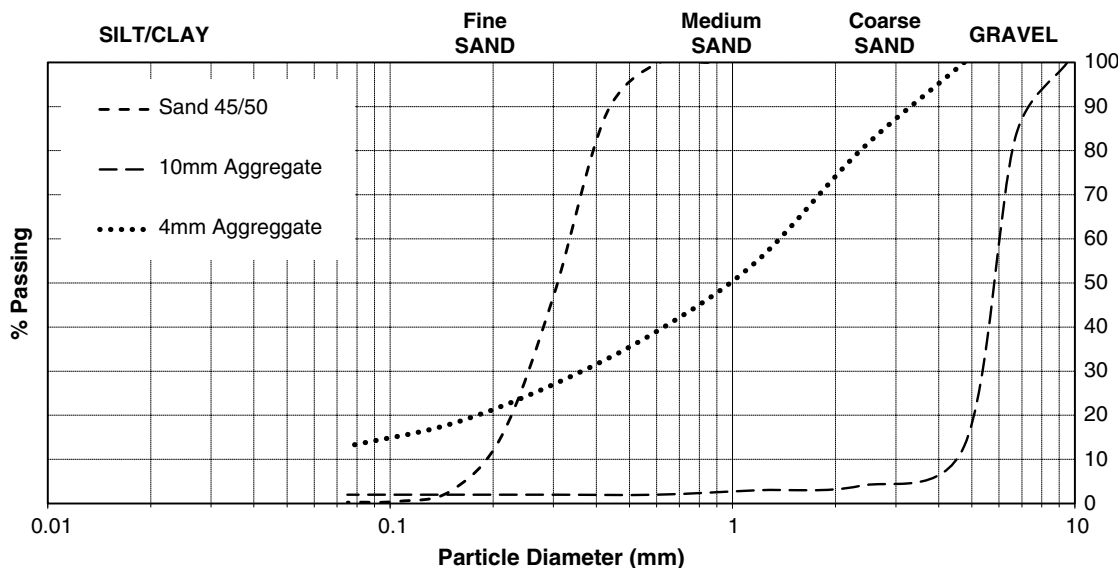


Fig. 1. Grading curve of natural aggregates and sand.

With the positive outcome of this research, specifically on the high-temperature residual properties of LWSCC, it may promote the use of LWAs as an alternative to normal aggregates, thereby ensuring the sustainable use of construction material.

Experimental Study

Materials

The materials used are broadly classified as binders, aggregates, and admixtures.

Cement

In this experimental study, similar to Aslani et al. (2018a, b), general-purpose cement (GPC) in accordance with AS3972 (AS 2010a) Type GP was used. The GPC was obtained from Cement Australia and contained up to 7.5% limestone mineral addition. The chemical, physical, and mechanical properties of the cement used in the experiment are shown in Table 1, and these properties adhere to the limiting values or permissible limits specified in AS 2450.2, 3, 4, 5, 7, 8, 9, 11, 13, and 14 (AS 1994).

Fly Ash

Fly ash particles are of similar size to cement particles; however, due to their spherical glassy shape, they have shown to improve the workability of concrete (Taylor 2013; Aslani et al. 2018a, b). Grade 1 fly ash complying with the requirements of AS3582.1 (AS 2001) was used in this experimental study similar to Aslani et al. (2018a, b). The chemical and physical properties of fly ash are given in Table 2, and these properties adhere to the limiting values or permissible limits specified in AS 2350.2 (AS 2006) and AS 3583.1, 2, 3, 5, 6, and 13 (AS 2016).

Ground Granulated Blast Furnace Slag

Ground granulated blast furnace slag (GGBFS) was used as a supplementary cementitious material similar to that used in Aslani et al. (2018a, b). GGBFS can delay setting time, and strength gain is generally slower at early ages; however, it develops a higher overall strength (Ries et al. 2003; Aslani et al. 2018a, b). GGBFS complies with AS 3582.2 (AS 2001). The properties of GGBFS are shown in Table 3.

Table 12. Chemical properties of perlite aggregates

Chemical property	Value
Silica	74%
Aluminum oxide	14%
Ferric oxide	1%
Calcium oxide	1.30%
Magnesium oxide	0.30%
Sodium oxide	3%
Potassium oxide	4%
Titanium oxide	0.10%
Heavy metals	Trace
Sulfate	Trace
Moisture	0.30%
Organic content	<0.1%

Table 13. Perlite aggregate distribution

Sieve size (mm)	Percentage retained
4.75	25–40
3.35	80–90
1.18	98–100

Table 14. Physical properties of perlite aggregates

Physical property	Value
Specific gravity	0.055–0.3
Color	Off white
Fusion point	1,250–1,340°C
Softening point	871–1,093°C

Silica Fume

The silica fume used in this experiment was tested under ASTM C1240 (ASTM 2005) and AS3582.3 (AS 1994), similarly to Aslani et al. (2018a, b). Silica fume consists of spherical glass-shaped particles that are much finer than cement particles. Its greater surface area makes it highly reactive and can provide a high early strength gain and low concrete permeability and reduce the probability of

Table 15. Scoria aggregate distribution

Sieve size (mm)	Percentage passing
13.2	100
9.5	76
6.7	14
4.75	7
2.36	7
0.075	2

Table 16. Physical properties of scoria aggregates

Physical property	Value
Apparent particle density	2.15 t/m ³
Dry particle density	1.71 t/m ³
SSD density	1.91 t/m ³
Water absorption	11.90%

bleeding (Taylor 2013; Aslani et al. 2018a, b). The chemical and physical properties of silica fume are given in Table 4.

Natural Aggregates

In this study, as in Aslani et al. (2018a, b), 10 and < 4 mm natural crushed sandstone aggregates were used as coarse and fine natural aggregates, respectively. Fine AFS 45-50 silica sand obtained from Rocla Quarry Products, Western Australia, was used in this experiment. The sampling methods and testing of these aggregates were done according to AS 1141 (AS 1974). Results are shown in

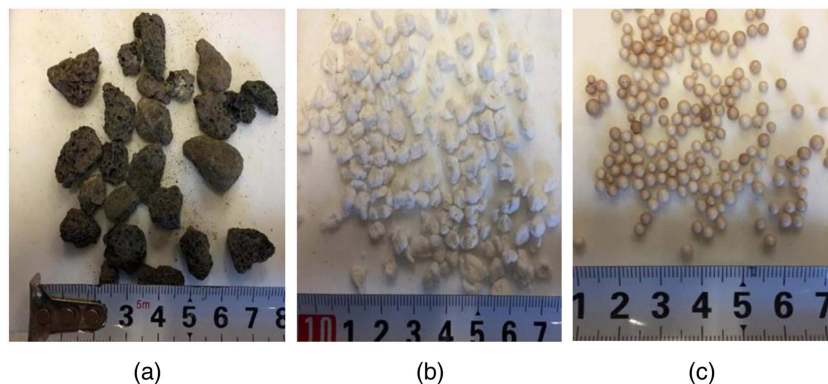
Tables 5–11, and the particle grading distribution can be found in Fig. 1.

Lightweight Aggregates

Perlite, scoria, and polystyrene (called BST) aggregates were used as LWAs in this experimental study. They are classified under lightweight or ultra-LWAs in accordance with AS2758.1 (AS 1998). Chemically coated BST aggregates were used in this experiment as an ultra-LWA as a replacement of fine natural aggregates. These BST aggregates are trademarked and distributed as BST in Australia and have traditionally been used as cement filler in the production of lightweight concrete. They have the following advantages: (a) light weight and high strength, (b) excellent fire resistance, (c) thermal and acoustic insulation, (d) low water permeability, (e) flexibility, and (f) ease of pumping and placement. Expanded perlite aggregates are natural siliceous volcanic rocks that are sourced from New Zealand; however, they are readily and commercially available in Australia. The properties of perlite aggregates are presented in Tables 12–14. Scoria is a natural volcanic aggregate and was used as a replacement of natural coarse aggregates. The properties of 10 mm scoria aggregates are presented in Tables 15 and 16 and photographs of the aggregates can be seen in Fig. 2.

Chemical Admixtures

In this experimental study, the SP complies with AS 1478.1 (AS 2000), which was a Type SN chemical admixture. It is designed to lower the viscosity and yield stress of fresh concrete, thereby improving the flow properties of concrete. The SP that was used in this project significantly improved the rheological behavior of

**Fig. 2.** LWAs: (a) scoria; (b) perlite; and (c) BST.**Table 17.** Mix proportions

Mix	Replacement (%)	Binders (kg/m ³)					Aggregates (kg/m ³)					Admixtures (L/m ³)				
		Cement	Fly Ash	Slag	Silica fume	Total cementitious	Water	Fine aggregate (4 mm)	Fine sand	Coarse aggregates (10 mm)	Scoria (10 mm)	Perlite	BST	SP	HRWRA	VMA
M1	50	180	135	101	34	450	202.5	554	363	379	215	—	—	2.5	0.75	1.65
M2	100	180	135	101	34	450	202.5	577	377	—	448	—	—	2.5	0.75	1.65
M3	50	180	135	101	34	450	202.5	287	385	786	—	54	—	2.8	0.75	1.5
M4	100	160	135	101	34	450	202.5	0	385	806	—	111	—	2.8	0.75	1.7
M5	20	160	135	101	34	450	202.5	456	373	781	—	—	2	2.4	0.75	2
M6	30	180	135	101	34	450	202.5	388	363	759	—	—	3	2.4	0.75	2
M7	50	180	135	101	34	450	135	554	363	379	215	—	—	3	0.75	1.65
M8	50	180	135	101	34	450	90	554	363	379	215	—	—	3.1	0.75	1.65

Note: BST = perlite, scoria, and polystyrene; HRWRA = high-range water reducer admixture; SP = superplasticizer; and VMA = viscosity-modifying admixture.

concrete, resulting in lower viscosity and yield stress, coupled with improved workability retention. High-range water reducer admixture (HRWRA) was used that satisfies Type HWR according to AS1478.1. HRWRA greatly improves cement dispersion and provides flowable concrete with greatly reduced water demand. Throughout this study, VMA was used and is required to control the stability and segregation resistance of SCC. VMA conforms with AS1478 (AS 2000) for Type SN admixtures.

Table 18. Fresh property test results

Mix	Slump flow diameter (mm)	J-ring diameter (mm)	T ₅₀₀ (s)	J-ring height difference (mm)	Density (kg/m ³)
M1	645	587.5	1.51	32	2,075.65
M2	630	565	2	45	2,033.48
M3	605	570	1.07	14	2,182.84
M4	595	550	1	45	2,128.35
M5	740	725	1.16	25	2,123.14
M6	750	720	1	23	2,076.71
M7	700	625	5.5	35	2,208.49
M8	675	590	6.5	42	2,211.22

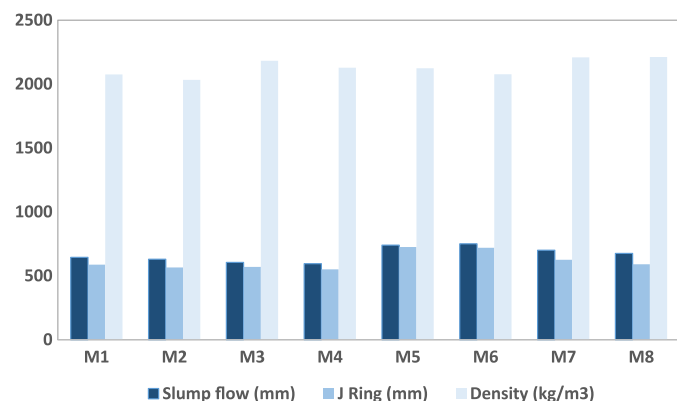


Fig. 3. Fresh property test results.

Mix Proportions

The mix design set in this study was obtained from the earlier research carried out at the University of Western Australia by Law Yim Wan et al. (2018). The mix design set was based on a control mix that had a 450 kg/m³ binder content and a 0.45 water-to-binder ratio; these were held constant throughout the experimental study. The binder composition of the control mixes consisted of 40% cement, 32.5% fly ash, 22.5% GGBFS, and 7.5% silica fume by volume.

Eight different mixes were prepared to investigate the high-temperature behavior and performance of LWSCC incorporating perlite, scoria, and BST aggregates, M1–M6 of normal strength [water/cement (w/c) = 0.45] and M7 and M8 of high strength (w/c = 0.3 and 0.2). The ingredients of each mix are presented in Table 17. Because SCC is very sensitive to aggregate size and grading, natural aggregates were replaced with LWAs of similar size. Therefore, using the control mix, natural coarse aggregates were replaced with scoria (SCR) at 50% and 100% replacement by volume for normal- and high-strength LWSCC; these mixes are M1, M2, M7, and M8. Perlite (PER) aggregates replaced natural fine aggregates at 50% and 100% replacement; these mixes are M3 and M4. Also, in two other mixes, natural fine aggregates were replaced with polystyrene (BST) aggregates at 20% and 30% replacement; these mixes are M5 and M6.

Sampling and Curing Conditions

Prior to mixing, some of the materials required pretreatment. LWAs (scoria, perlite, and BST) were wetted for 24 h before being mixed. This was necessary because the aggregates in a later stage absorbed water, which would alter the workability of the concrete and its strength. The pretreatment and water absorption of the aggregates are explained in detail in Law Yim Wan et al. (2018). For hardened property tests at 20°C, 100°C, 300°C, 600°C, and 900°C, each mix required 45 φ100 × 200 mm cylindrical molds for compressive and tensile strength and stress-strain tests. The specimens were prepared by pouring the concrete directly into the molds without compacting, demolded after 24 h, and allowed to cure until the testing age. The specimens were cured in a controlled humidifying room at a temperature of 20 ± 2°C. Their weights and densities were measured and recorded under saturated surface dry (SSD) conditions.



Fig. 4. Scoria aggregate distribution of (a) 50%; and (b) 100% replacements.

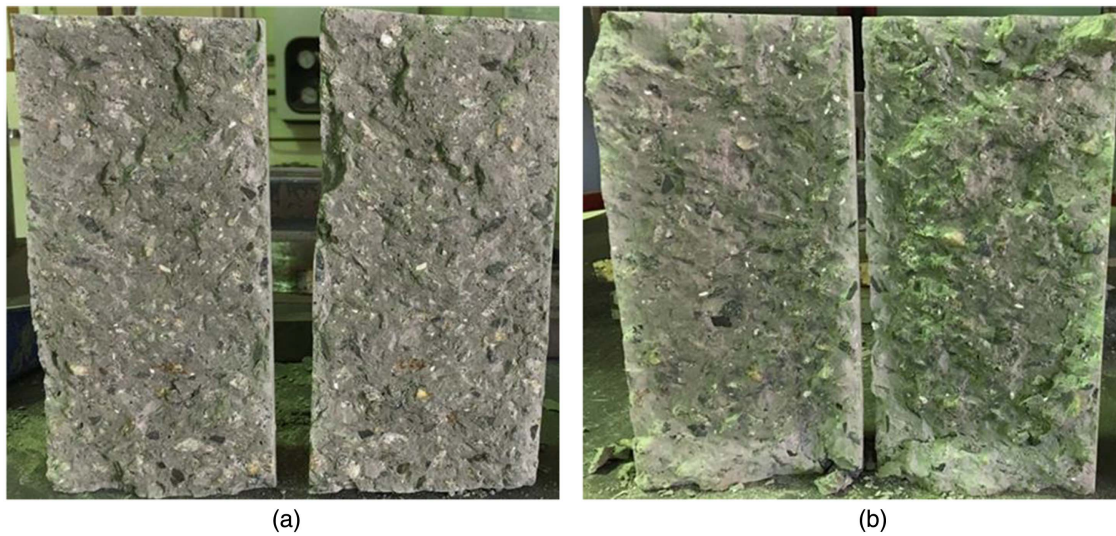


Fig. 5. Perlite aggregate distribution of (a) 50%; and (b) 100% replacements.



Fig. 6. BST aggregate distribution of (a) 20%; and (b) 30% replacements.

Mix	100°C	300°C	600°C	900°C		Mix	100°C	300°C	600°C	900°C	
M1	No visible impact on the surface of specimen	No visible impact on the surface of specimen	No visible impact on the surface of specimen			M5	No visible impact on the surface of specimen	No visible impact on the surface of specimen	No visible impact on the surface of specimen		
M2	No visible impact on the surface of specimen	No visible impact on the surface of specimen	No visible impact on the surface of specimen			M6	No visible impact on the surface of specimen	No visible impact on the surface of specimen	No visible impact on the surface of specimen		
M3	No visible impact on the surface of specimen	No visible impact on the surface of specimen	No visible impact on the surface of specimen			M7	No visible impact on the surface of specimen	No visible impact on the surface of specimen		N/A	
M4	No visible impact on the surface of specimen	No visible impact on the surface of specimen	No visible impact on the surface of specimen			M8	No visible impact on the surface of specimen		N/A	N/A	

(a)

(b)

Fig. 7. Performance of concrete mixtures at high temperatures.

Sample Test Methods

The cylinders were then stored at room temperature until they reached a constant dry weight. Three representative concrete cylinder specimens from each batch were chosen, and three cylinder specimens were tested at every temperature. The mechanical properties of the mixes were measured by heating the cylinders at 5°C/min to temperatures of 100°C, 300°C, 600°C, and 900°C, similar to Bastami et al. (2014). They were kept for 1 h and the cylinders were then slowly cooled to room temperature for 24 h before the residual strength tests were conducted.

The time-temperature curve of the furnace almost fits the standard curve recommended by ISO Fire 834 (ISO 1999). The heating rate of the experimental curve was slightly less than the ISO recommendation, which was a limitation imposed by available equipment. It is likely that this had only a minimal effect on the results

since the duration of exposure at the maximum temperature was 1 h (Bastami et al. 2014).

In this experiment, similar to Aslani et al. (2018a, b), the hardened properties of the concrete were assessed by its compressive strength, tensile strength, and stress-strain behavior. For compressive strength tests, three $\phi 100 \times 200$ mm cylindrical specimens were tested at 28 days. The testing procedure follows AS1012.14 (AS 1991), and the cylinders were loaded at a rate of 0.2 kN/s until failure. The three $\phi 100 \times 200$ mm cylinders tested for compressive strength at 28 days were weighed and their dimensions measured to obtain their hardened density in accordance with AS3582.3 (AS 1994).

Furthermore, similar to Aslani et al. (2018a, b), three $\phi 100 \times 200$ mm specimens were tested for their compressive stress-strain curve at 28 days, and they were attached with 60 mm horizontal and 60 mm vertical strain gauges to obtain the stress-strain behavior as

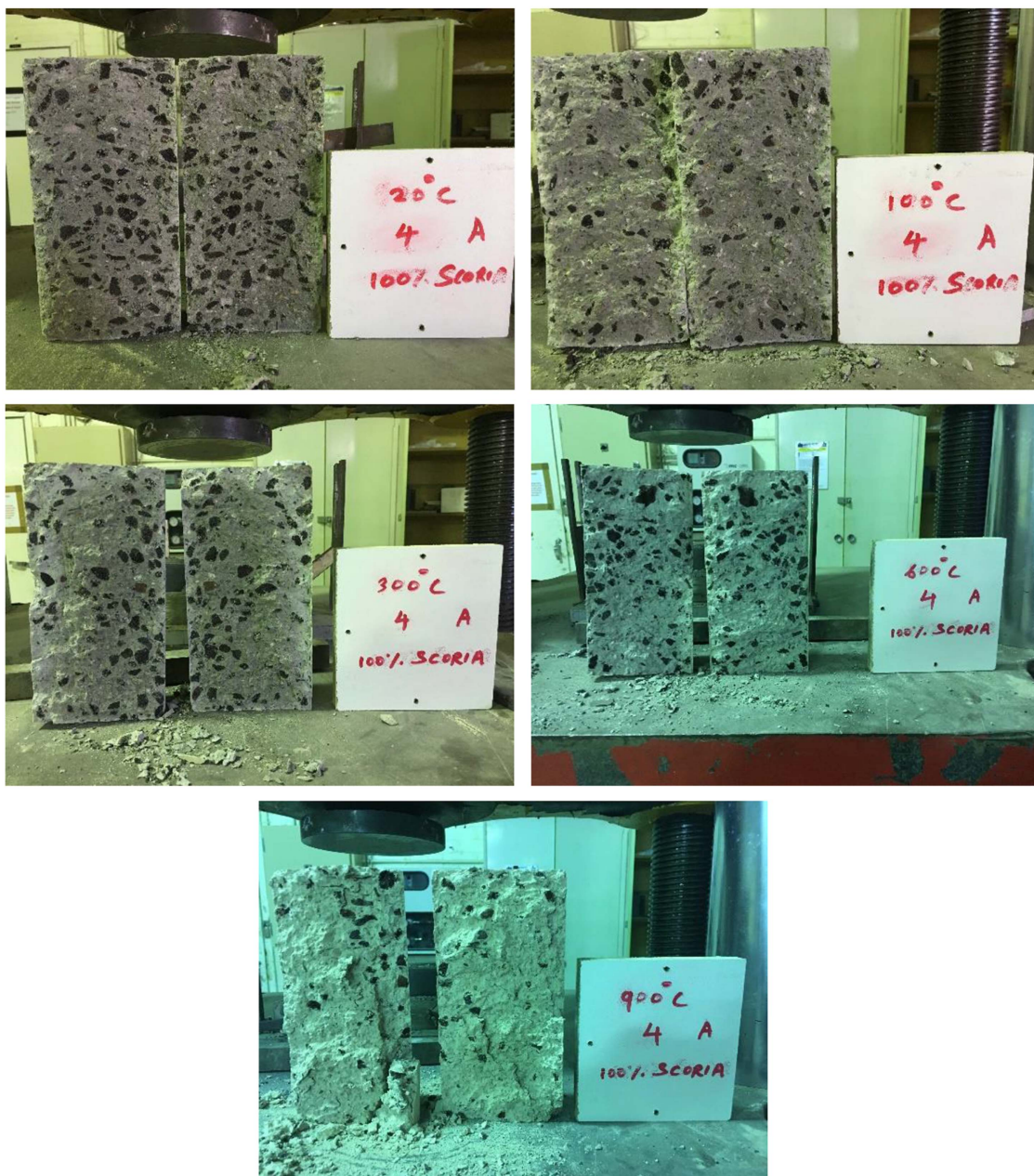


Fig. 8. Effect of high temperatures on M2 (100% scoria).

per AS.1012.17 (AS 1997). A splitting tensile test was conducted on three $\phi 100 \times 200$ mm cylindrical specimens at each testing age of 28 days in accordance with AS1012.10 (AS 2010b). The specimens were loaded at a rate of 1.5 ± 0.5 kN/s until failure, similar to Aslani et al. (2018a, b).

Properties of Fresh Concrete

The fresh properties of SCC, similar to Aslani et al. (2018a, b), were assessed through the tests specified under the guidelines and SCC criteria defined by EFNARC (2002, 2005). These experimental tests assess the flowability, viscosity, passing ability, and resistance to segregation. The slump flow test, T_{500} , and J-ring test were conducted using an Abrams cone in accordance with AS1012.3.5 (AS 2015). The slump flow diameter and the time to reach

500 mm (T_{500}) were measured. In the J-ring test, the diameter and the J-ring height difference were measured.

Spalling and Mass Loss

The mass of concrete decreases with increasing temperature due to a loss of moisture. The retention of the mass of concrete at elevated temperatures is highly influenced by the type of aggregate used (Kodur 2014). The measurement of the mass of the specimens before and after high-temperature exposure was carried out as per AS 1012.12.1 (AS 2014).

Spalling is defined as the breaking up of parts of concrete from the surface of concrete exposed to high temperature (Kodur 2014). After heating, the sample was physically observed for the formation of cracks, bubbles, holes, and loss of parts. Spalling of the specimens was measured following exposure to high temperatures.

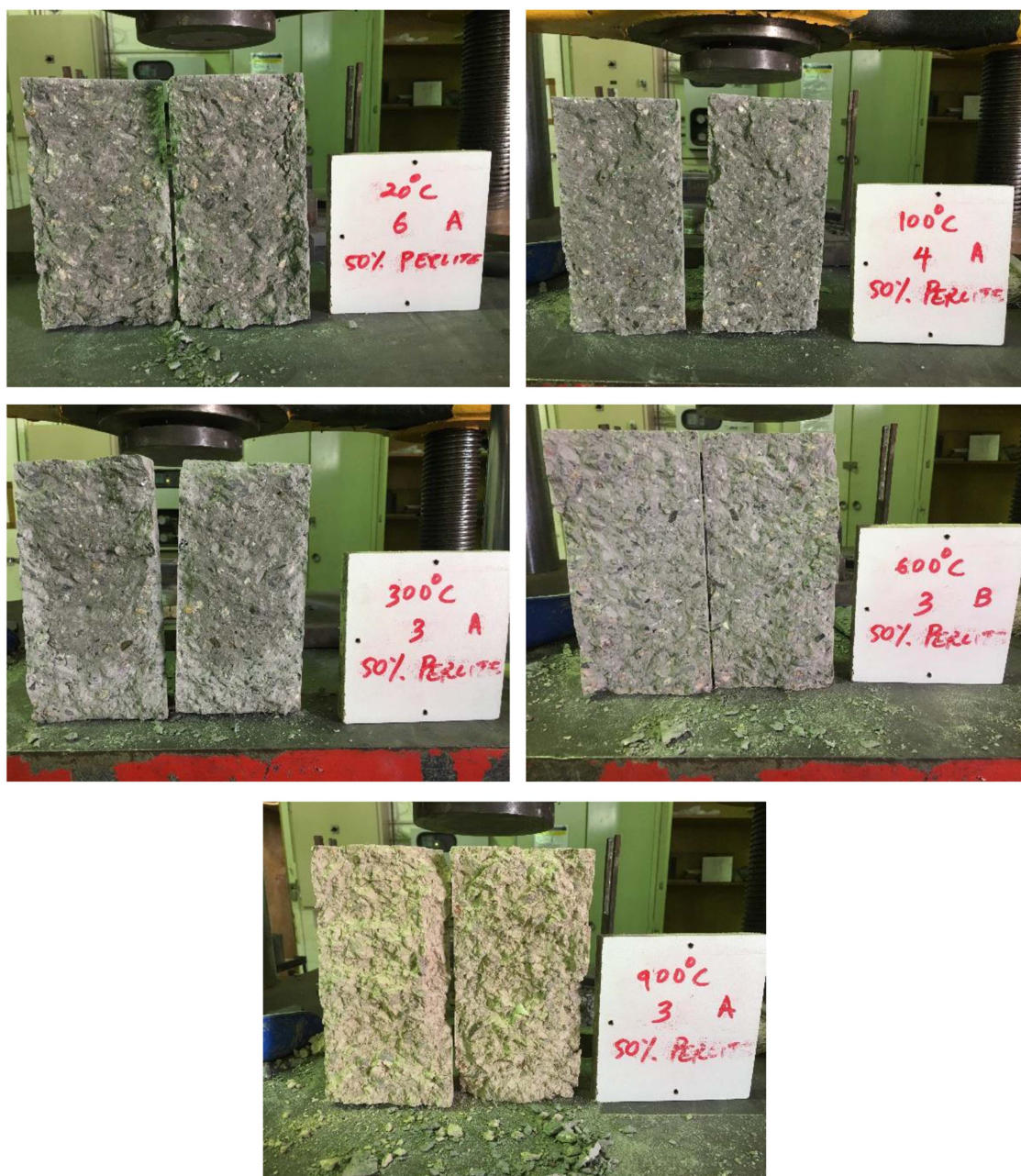


Fig. 9. Effect of high temperatures on M3 (50% perlite).

Experimental Results

Properties of Fresh Concrete

The results of the tests of fresh properties, including the slump flow test (slump flow diameter and time taken to reach 500 mm diameter, T_{500}) and the J-ring test (flow diameter and J-ring height difference), are presented in Table 18 and Fig. 3.

At a higher binder content, a sufficient slump flow diameter characteristic of SCC can be achieved with a lower dose of SP and without any viscosity-modifying agent present. The increase in binder content increases the plastic viscosity of the mixture, thereby controlling its segregation resistance, whereas the use of lower binder content requires the use of VMA to provide additional plastic viscosity for purposes of stability.

Fresh Properties of Scoria Mixes (M1, M2, M7, and M8)

All M1, M2, M7, and M8 mixes satisfied SCC criteria for flowability, as indicated by the slump flow results (Table 18 and Fig. 3). However, these mixes showed a decrease in passing ability at increasing scoria replacements, as indicated by the J-ring height difference. The aggregate distributions of the mixes containing scoria are presented in Fig. 4.

The improved workability could also be a result of the ambiguity in preparing the scoria aggregates under SSD conditions. The scoria aggregates were prewetted for 24 h and left to dry for 24 h. However, the condition of the aggregates could have been affected by the humidity and temperature when drying. This increase in water content might have caused an associated decrease in density. Densities of 2,075.65, 2,033.48, 2,208.49, and 2,211.22 kg/m³ were captured for Mixes M1, M2, M7, and M8, respectively.

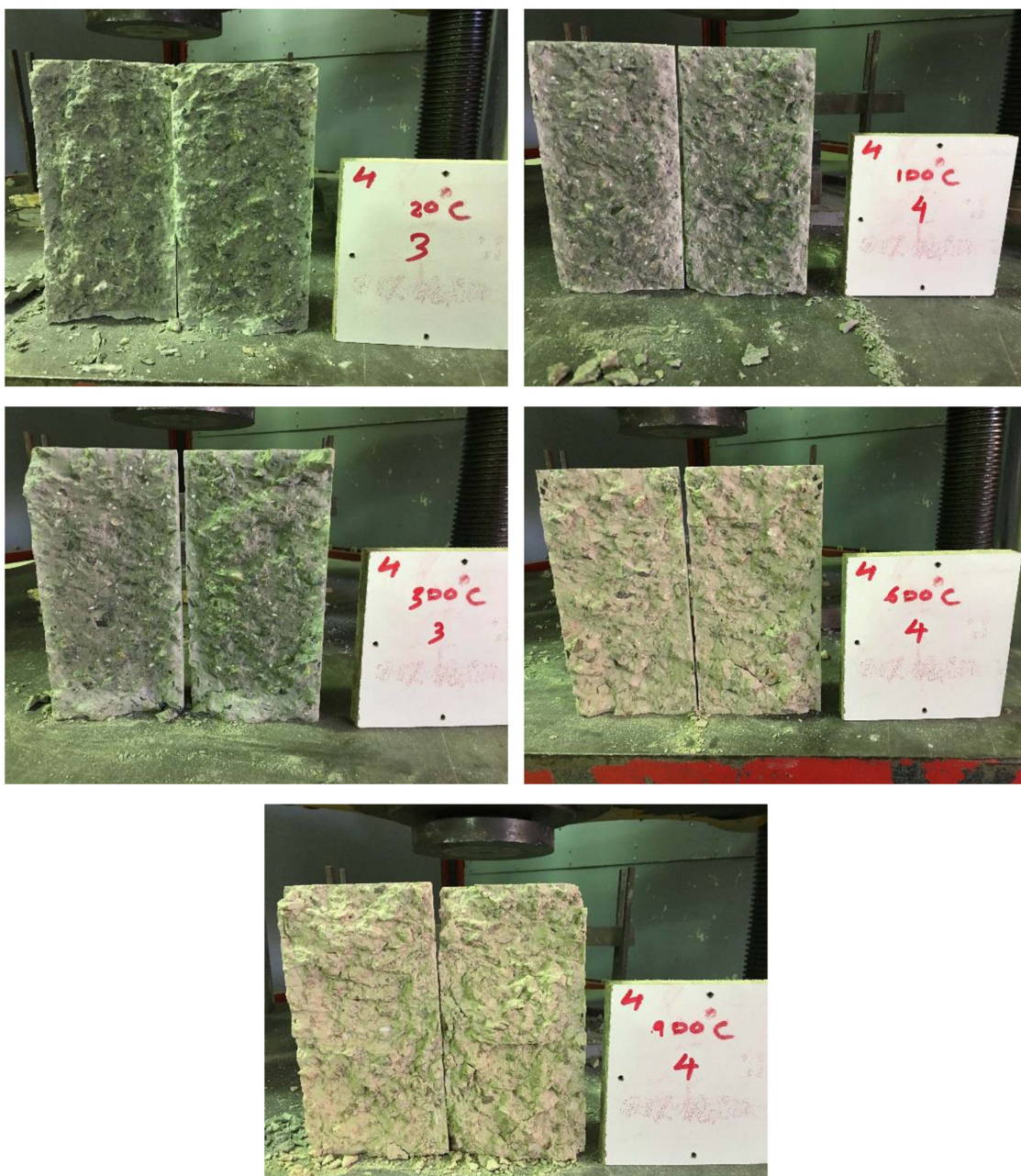


Fig. 10. Effect of high temperatures on M4 (100% perlite).

Fresh Properties of Perlite Mixes (M3 and M4)

During the pretreatment of the perlite aggregates, it was noticed that perlite aggregates expanded in size as water was absorbed. However, when treated and dried to SSD conditions, the volume of the aggregates would remain at its expanded size. Once the perlite aggregates entered the mix, the aggregates were crushed and compressed back to a smaller size that was similar to its original dry conditions. As the aggregates were compressed, excess pore water in the aggregates was released. This effect caused the mixture to have a higher water content, thereby decreasing the viscosity and yield point. This explains the lack of homogeneity in the T_{500} times recorded and the reduction in SP used in mixes containing a higher perlite content. The aggregate distributions of the mixes containing perlite are presented in Fig. 5.

Overall, the M3 and M4 perlite mixes satisfied the fresh property criteria of SCC in terms of flowability and passing ability,

as shown in Table 18 and Fig. 3. However, the volatility of the T_{500} times needs to be addressed because the low mix time indicates a low viscosity, which could increase the possibility of segregation. Densities of 2,182.84 and 2,128.35 kg/m³ were captured for Mixes M3 and M4, respectively.

Fresh Properties of BST Mixes (M5 and M6)

BST aggregates were highly prone to segregation due to their ultralightweight nature. As a result, less SP was used in comparison to the control mix and larger doses of VMA were required to control segregation, this effect being especially significant with increasing amounts of BST. The aggregate distributions of the mixes containing BST are presented in Fig. 6. There was a significant decrease in workability across all fresh property tests as the percentage replacement of BST is increased, as shown in Table 18 and Fig. 3. Densities of 2,123.14 and 2,076.71 kg/m³ were captured for Mixes M5 and M6, respectively.

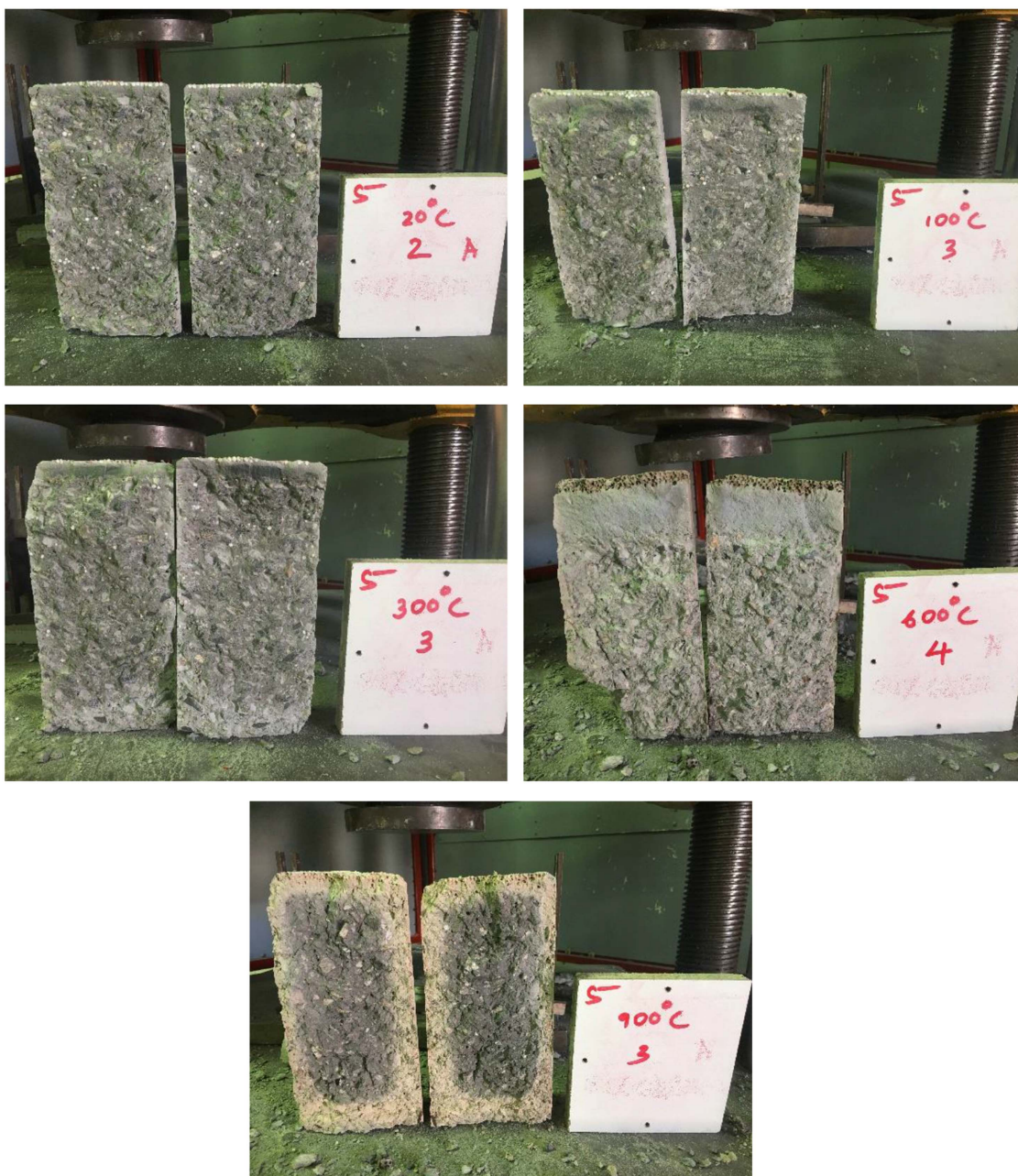


Fig. 11. Effect of high temperatures on M5 (20% BST).

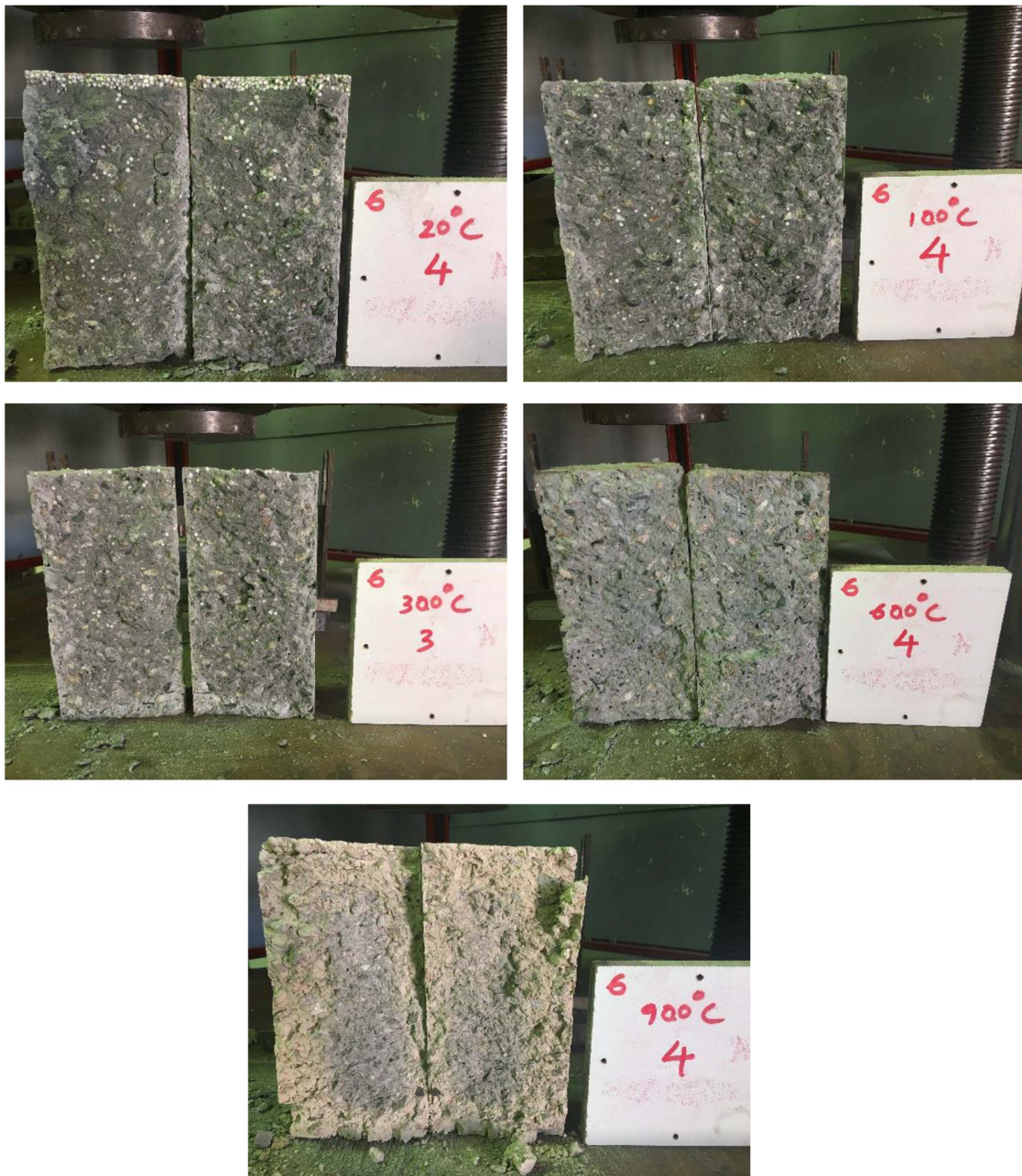


Fig. 12. Effect of high temperatures on M6 (30% BST).

Spalling and Mass Loss

The extent, harshness, and nature of spalling varied. Spalling was considered insignificant when only surface pitting occurred. But spalling can affect the fire resistance and load-bearing capacity of a structural element if it exposes the core and reinforcing steel or tendons to a rapid rise in temperature. Therefore, the consequences of spalling depend upon the application for which the concrete is used (Aslani and Bastami 2011; Aslani and Samali 2013, 2014a, b, 2015; Aslani 2013b, 2018; Bastami et al. 2014). In this study, spalling was observed (Figs. 7–14).

M1, M2, M3, M4, M5, and M6 specimens experienced minor spalling when heated to more than 600°C. Also, M7 and M8 specimens experienced severe spalling when heated to more than 300°C. Figs. 7–14 show the performance and spalling of the specimens at 20°C, 100°C, 300°C, 600°C, and 900°C.

Fig. 15 shows an increase in mass loss with increasing temperature. The loss is higher in M2 owing to the higher content of scoria, which decomposes at higher temperatures, losing mass. The loss ranged from a minimum of 0.8% at 100°C to a maximum of 13.1% at 900°C. The average mass loss for Mixes M1 and M2 was 1.06%, 2.52%, 10.17%, and 11.80% at 100°C, 300°C, 600°C, and 900°C, respectively.

In the case of mass loss, the M4 mix exceeded that of the M3 mix during the heating process, so perlite aggregates might have undergone more decomposition (Fig. 15 and Table 19). The mass loss ranged from 0.7% to 13.3%. The average mass loss for the M3 and M4 mixes was 1.03%, 4.85%, 10.38%, and 11.63% at 100°C, 300°C, 600°C, and 900°C, respectively.

As shown in Fig. 15 and Table 19, M5 and M6, with BST aggregates, showed less mass loss compared to the scoria and perlite mixes. This indicates that BST aggregates are highly resistant to

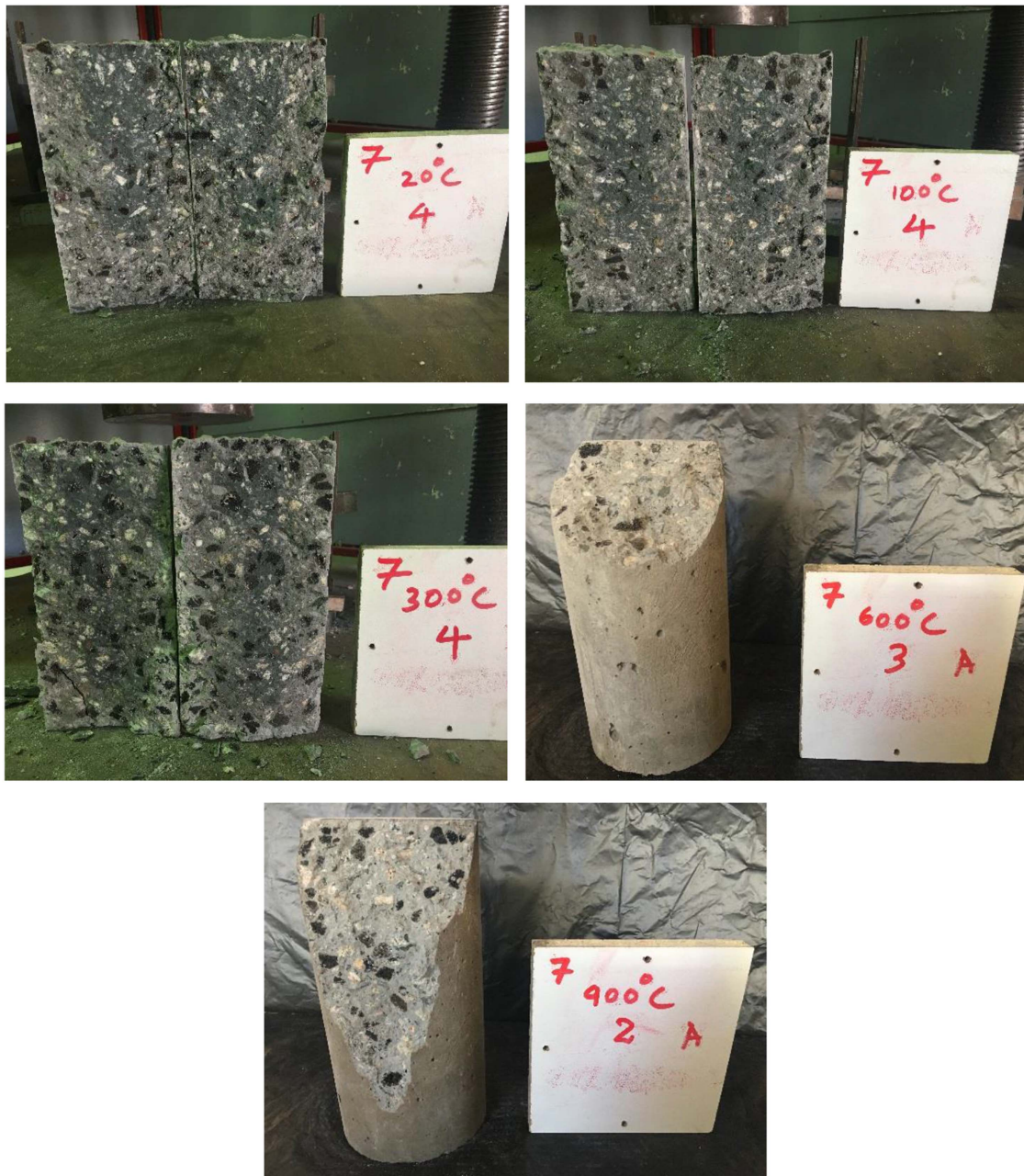


Fig. 13. Effect of high temperatures on M7 (50% scoria).

heat. The average mass loss for the M5 and M6 mixes was 0.53%, 2.29%, 7.75%, and 9.50% at 100°C, 300°C, 600°C, and 900°C, respectively.

Mass loss was 1.69% for Mix M7 at 300°C and 0.3% for Mix M8 at 100°C. The average mass loss for Mixes M7 and M8 was 0.28% and 1.69% at 100°C and 300°C, respectively.

Hardened Properties

The residual compressive strength, residual tensile strength, residual modulus of elasticity (MOE), and mass loss are given in Tables 20–22 and Figs. 15–18. The results of Mixes M7 and M8 at some temperatures are not available owing to the explosion of the sample, so that factor could not be tested. The results revealed that in the majority of mixes, the highest strength both in compression and tension was achieved at 100°C and the minimum at 900°C.

The strength decreased as temperature rose above 100°C. The strength of concrete is marginally affected by temperature up to 300°C, followed by a sharp decline above 300°C.

Hardened Properties of Scoria Mixes (M1, M2, M7, and M8)

Tables 20–22 and Figs. 16–18 show the hardened properties of scoria mixes at high temperatures. A maximum compressive residual strength of 39.14 and 34.5 MPa was obtained for M1 and M2, respectively. The maximum residual tensile strength was 3.24 and 3 MPa for M1 and M2, respectively. As shown in Fig. 16, the residual compressive strength was higher in M1 compared to M2 because of the low percentage of LWA scoria, indicating that LWAs are weak in compression and a higher percentage of LWA content in concrete would reduce the compressive strength. The average difference was found to be 12.54%, while the converse holds in



Fig. 14. Effect of high temperatures on M8 (50% scoria).

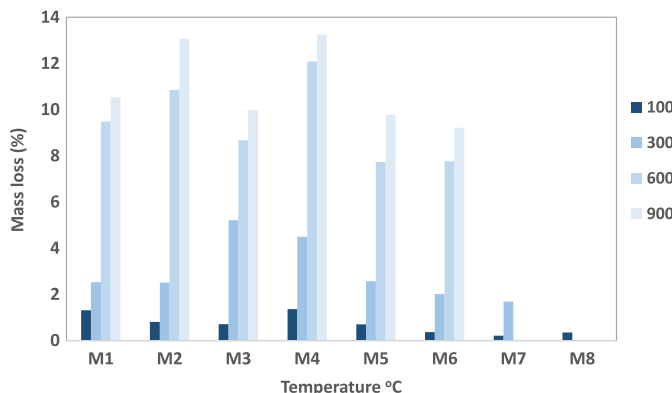


Fig. 15. Mass loss versus temperature.

the case of residual tensile strength. Fig. 17 shows that the residual tensile strength is higher in M2 compared to M1, which indicates that scoria has good tensile strength. An average difference of 38.30% was observed in tensile results which is high compared

to strength loss in compressive results. This indicates that temperature has a significant effect on the tensile strength of concrete. This indicates that temperature has a large effect on the tensile strength of concrete.

The trend of the MOE (Fig. 18) is similar to that of compressive strength (Fig. 16). The maximum MOE was achieved at 100°C and decreased as temperature increased. This is mainly because MOE is a function of the compressive strength and density of concrete. The maximum MOE of the M1 mix was 25.99 GPa at 100°C, while that of the M2 mix was 23.85 GPa at 100°C.

The results for the M7 mix are given up to 300°C and for the M8 mix up to 100°C (Tables 20–22 and Figs. 16–18). This was due to the explosion of the samples. High-strength concrete is more susceptible to heat and tends to explode at high temperatures. This is mainly due to a low w/c ratio and higher density. The M7 mix achieved a high strength of 60.67 MPa, and M8 achieved a strength of 79.18 MPa, which satisfies the requirements for high-strength concrete. The maximum compressive strengths were obtained at 100°C for the M7 and M8 mixes, 63.27 and 79.30 MPa, respectively. Fig. 18 and Table 22 show that the maximum MOE was obtained by the M8 mix at a value of 34.70 GPa at 100°C and by the M7 mix at a value of 32.27 GPa at 100°C.

Table 19. Mass loss (percentage) by temperature

Temperature (°C)	Mass loss (%)								Average
	M1	M2	M3	M4	M5	M6	M7	M8	
100	1.31	0.80	0.71	1.36	0.70	0.37	0.21	0.35	0.78
300	2.52	2.51	5.21	4.50	2.57	2.01	1.69	—	3.00
600	9.48	10.85	8.67	12.09	7.73	7.76	—	—	9.43
900	10.53	13.07	10.00	13.26	9.78	9.21	—	—	10.98

Table 20. Residual compressive strength versus temperature

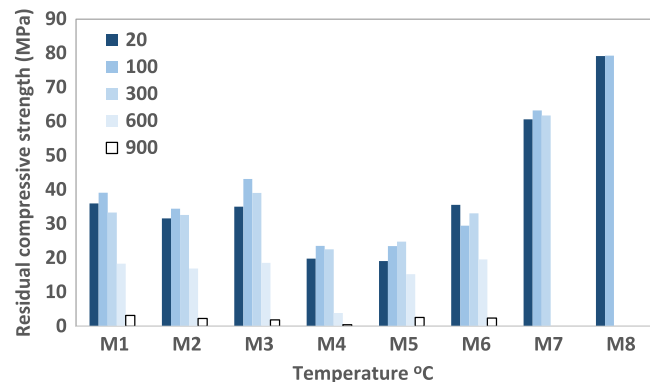
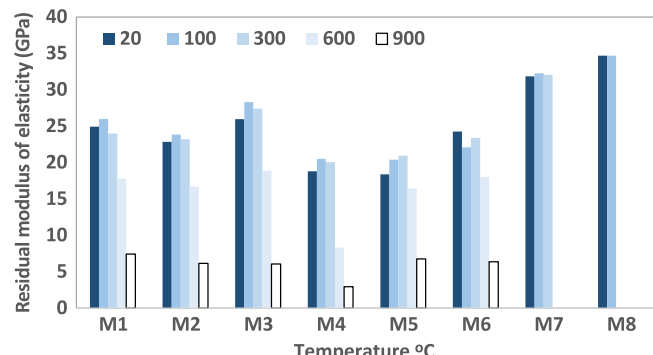
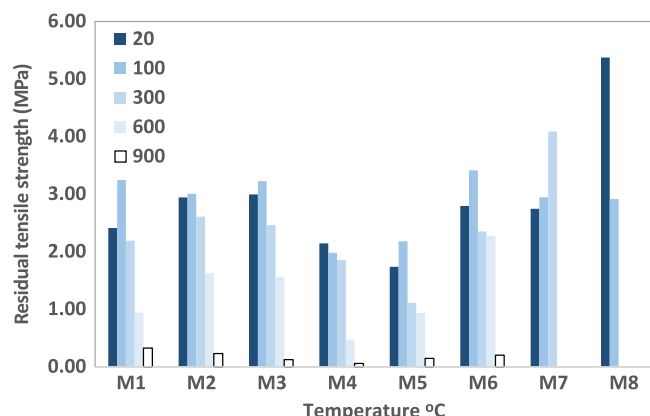
Temperature (°C)	28-day compressive strength (MPa)							
	M1	M2	M3	M4	M5	M6	M7	M8
20	36.01 ± 0.98	31.61 ± 1.10	35.08 ± 0.96	19.84 ± 0.92	19.10 ± 1.21	35.59 ± 1.51	60.67 ± 0.98	79.18 ± 3.12
100	39.14 ± 1.01	34.45 ± 1.23	43.17 ± 1.17	23.56 ± 1.23	23.53 ± 0.85	29.49 ± 0.86	63.27 ± 3.20	79.3 ± 2.50
300	33.33 ± 0.84	32.66 ± 0.96	39.07 ± 0.93	22.56 ± 2.10	24.83 ± 1.2	33.11 ± 0.96	61.79 ± 2.40	—
600	18.38 ± 0.76	16.95 ± 0.64	18.58 ± 1.32	3.89 ± 0.75	15.25 ± 0.77	19.60 ± 1.05	—	—
900	3.21 ± 0.83	2.29 ± 0.74	1.92 ± 0.96	0.49 ± 0.21	2.59 ± 0.45	2.45 ± 2.00	—	—

Table 21. Residual tensile strength versus temperature

Temperature (°C)	28-day tensile strength (MPa)							
	M1	M2	M3	M4	M5	M6	M7	M8
20	2.41 ± 0.14	2.94 ± 0.12	2.99 ± 0.23	2.15 ± 0.27	1.74 ± 0.19	2.80 ± 0.23	2.75 ± 0.41	5.38 ± 0.37
100	3.24 ± 0.23	3.00 ± 0.15	3.23 ± 0.12	1.98 ± 0.23	2.18 ± 0.13	3.41 ± 0.31	2.94 ± 0.32	2.91 ± 0.43
300	2.19 ± 0.34	2.61 ± 0.17	2.46 ± 0.25	1.86 ± 0.19	1.11 ± 0.32	2.35 ± 0.43	4.09 ± 0.36	—
600	0.94 ± 0.26	1.63 ± 0.23	1.56 ± 0.19	0.47 ± 0.11	0.94 ± 0.21	2.27 ± 0.20	—	—
900	0.32 ± 0.10	0.23 ± 0.10	0.13 ± 0.09	0.06 ± 0.03	0.14 ± 0.05	0.20 ± 0.07	—	—

Table 22. Residual modulus of elasticity versus temperature

Temperature (°C)	28-day modulus of elasticity (GPa)							
	M1	M2	M3	M4	M5	M6	M7	M8
20	24.93 ± 0.52	22.84 ± 0.76	25.97 ± 1.00	18.81 ± 1.10	18.39 ± 0.86	24.28 ± 2.10	31.86 ± 0.54	34.68 ± 0.98
100	25.99 ± 0.43	23.85 ± 0.88	28.32 ± 0.95	20.50 ± 0.94	20.41 ± 0.97	22.10 ± 1.12	32.27 ± 1.50	34.70 ± 1.12
300	23.99 ± 0.38	23.22 ± 0.68	27.41 ± 0.87	20.05 ± 0.87	20.96 ± 1.21	23.41 ± 1.09	32.03 ± 1.43	—
600	17.81 ± 0.59	16.73 ± 0.71	18.90 ± 0.67	8.32 ± 0.76	16.43 ± 0.87	18.02 ± 0.98	—	—
900	7.44 ± 0.70	6.15 ± 0.80	6.07 ± 0.55	2.94 ± 0.65	6.77 ± 0.76	6.37 ± 0.65	—	—

**Fig. 16.** Residual compressive strength versus temperature.**Fig. 18.** Residual MOE versus temperature.**Fig. 17.** Residual tensile strength versus temperature.**Hardened Properties of Perlite Mixes (M3 and M4)**

Tables 20–22 and Figs. 16–18 show the hardened properties of the perlite mixes at high temperatures. For Mix M3 with 50% perlite replacement, the maximum compressive residual strength obtained was 43.17 MPa at 100°C and the maximum compressive residual strength for the M4 mix with 100% replacement was 23.56 MPa at 100°C. The average difference between the scoria and perlite mixes indicates that perlite is weaker than scoria in terms of compressive strength. Regarding the residual tensile strength, the maximum strength obtained was 3.23 and 2.15 MPa for the M3 and M4 mixes, respectively.

As shown in Fig. 18 and Table 22, the maximum residual MOE of the M3 mix was greater than that of the M4 mix at all temperatures, which could be due to the presence of low percentages of perlite aggregates. The maximum MOE, obtained at 100°C, was 28.32 and 20.50 GPa for M3 and M4, respectively.

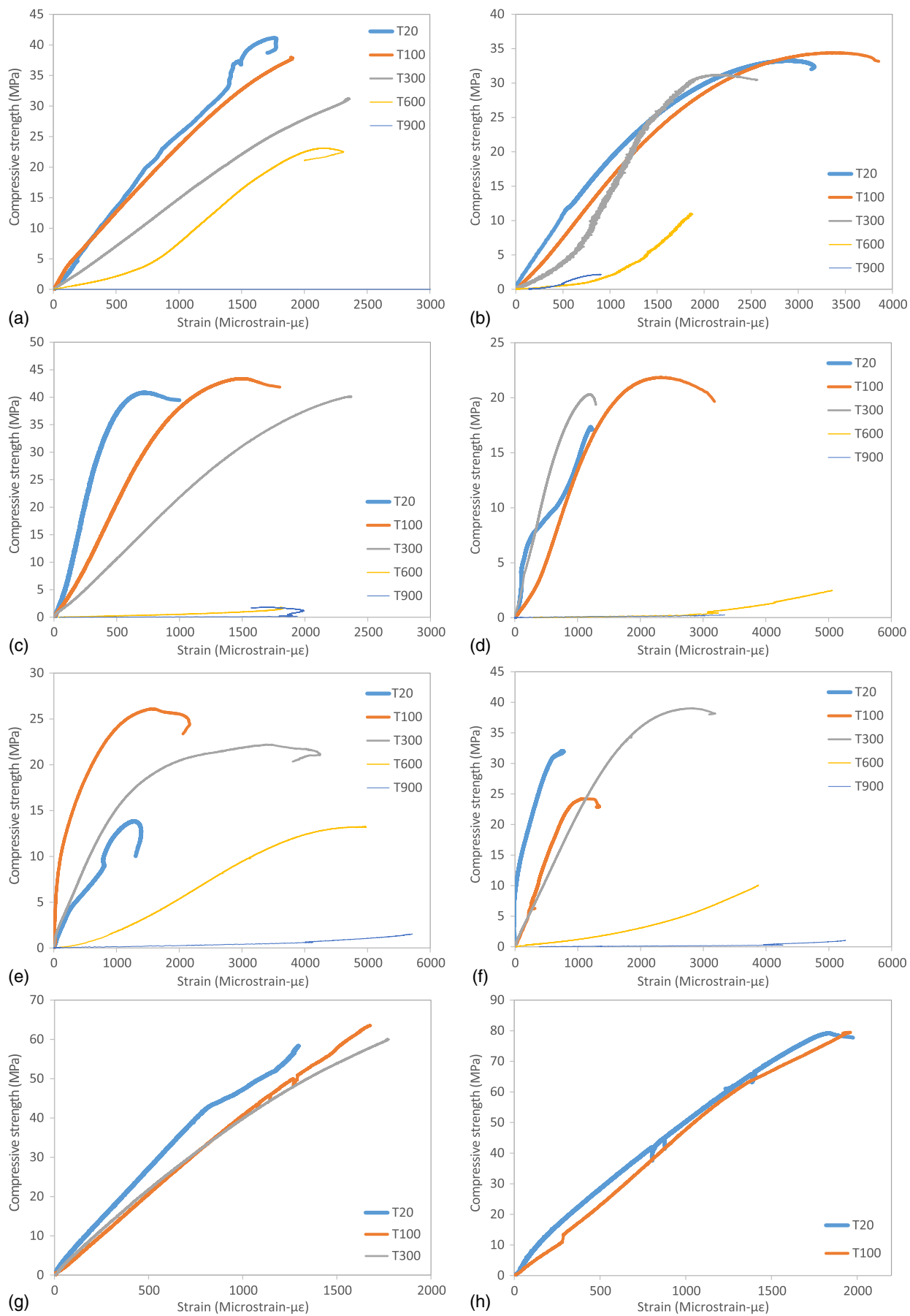


Fig. 19. Compressive stress-strain curve for mix: (a) M1; (b) M2; (c) M3; (d) M4; (e) M5; (f) M6; (g) M7; and (h) M8 at high temperatures.

Hardened Properties of BST Mixes (M5 and M6)

Tables 20–22 and Figs. 16–18 show the hardened properties of BST mixes at high temperatures. Overall performance was better in the M6 mix, which contained 30% BST. In terms of both compression and tension, the M6 mix performed better compared with the M5 mix. The maximum residual compressive strength for the M6 mix was 35.59 MPa at 20°C, and for the M6 mix it was 24.83 MPa at 300°C. The minimum residual compressive strength was achieved at 900°C with values of 2.59 and 2.45 MPa for the M5 and M6 mixes, respectively.

Also, the M5 and M6 mixes achieved their maximum residual tensile strength at 100°C with values of 2.18 MPa and 3.41 MPa, respectively (Fig. 17 and Table 21). The average difference between the tensile strengths of M5 and M6 was 57%, which is greater than replacements by scoria and perlite aggregates. This shows that the slight variation in the content of BST aggregates is important.

As in the case of compressive force, Mix M6 has a higher MOE compared to Mix M5.

As shown in Fig. 18 and Table 22, the maximum residual MOE of Mix M6 was greater than Mix M5; this could be due to the presence of higher percentages of BST aggregates. Mix M6 achieved its maximum MOE, 24.28 GPa, at 20°C, while M5's maximum MOE, 20.96 GPa, was achieved at 300°C.

Compressive Stress-Strain Behavior

The compressive stress-strain curves for mixes containing scoria, perlite, and BST are shown in Fig. 19. The figure shows that the M1 and M2 mixes exposed to high temperatures lost their structural integrity due to a decreasing compressive strength and stiffness, which led to easy deformation. The maximum strain was observed at a temperature of 900°C. In Fig. 19, the stress-strain curves at 600°C and 900°C are not consistent because the strain gauges could not be attached properly to the samples owing to their softness. The peak strain at 20°C for the M1 mix fell below a microstrain of 1,750, and for the M2 mix the peak strain at 20°C was almost 3,000 microstrain. Figs. 19(g and h) show that the compressive stress-strain curves for the M7 and M8 mixes are similar, except that for M7 the peak strain at 20°C falls below 1,500 microstrain and for M8 the peak strain at 20°C is almost 2,000 microstrain.

Figs. 19(c and d) show that the M3 and M4 mixes exposed to high temperature lost their structural integrity owing to a decreasing compressive strength and stiffness, which led to easy deformation. The strain was observed to be greater in the M4 mix, which may be attributed to a higher content of perlite compared to M3. The result is that the LWA has less compressive strength and can undergo more deformation than the natural aggregate. The peak strain at 20°C for the M3 mix falls below 750 microstrain and for the M4 mix the peak strain at 20°C is almost 1,200 microstrain.

Figs. 19(e and f) show that the M5 and M6 mixes, which contain respectively 20% and 30% BST aggregates, following a similar trend to mixes containing scoria and perlite aggregates at high temperatures. However, the M5 and M6 peak strains at 20°C are less than those of the scoria and perlite mixes. The peak strain at 20°C for the M5 mix exceeds 1,000 microstrain, and for the M6 mix the peak strain at 20°C is almost 500 microstrain.

Conclusions

The experimental study presented in this article may serve as a basis for developing and promoting the use of normal-strength lightweight self-compacting concrete (NSLWSCC) and high-strength lightweight self-compacting concrete (HSLWSCC) using three types of LWA (scoria, perlite, and polystyrene) in Australia.

In addition, the behavior of these concretes under elevated temperatures was studied. Most of the mixes prepared in this study satisfied both lightweight concrete classifications and SCC classifications. The results presented in this study reveals the following trends:

1. For NSLWSCC mixes with scoria replacements (M1 and M2):
 - a. Maximum strength (compressive/tensile) was achieved at 100°C.
 - b. Strength diminishes as temperature exceeds 100°C.
 - c. A higher percentage of scoria decreases compressive strength and increases tensile strength.
 - d. Minor spalling is observed only at 900°C.
2. For NSLWSCC mixes with perlite and BST replacements (M3, M4, M5, and M6):
 - a. Maximum strength (compressive/tensile) was achieved at 100°C.
 - b. Strength diminishes as temperature exceeds 100°C.
 - c. A higher percentage of perlite decreases both compressive and tensile strengths.
 - d. Less mass loss is observed for BST mixes (M5 and M6).
 - e. Peak strains in compressive stress-strain curves were less for BST mixes (M5 and M6).
 - f. Minor spalling is observed only at 900°C.
3. For HSLWSCC mixes with 50% scoria replacement (M7 and M8):
 - a. Maximum strength (compressive/tensile) is achieved at 300°C.
 - b. Explosion occurs at low temperature (300°C).
4. General observations:
 - a. The lower the density of the aggregate, the more prone it is to segregation resistance of LWSCC.
 - b. The maximum compressive strength among the NSLWSCC mixes was obtained in Mix M3 containing 50% perlite with a strength of 43.17 MPa.
 - c. The maximum tensile strength in NSLWSCC mixes was achieved in Mix M6 containing 30% BST with a strength of 3.41 MPa.
 - d. The maximum compressive strength among the HSLWSCC mixes was obtained in Mix M8 (50% scoria and w/c = 0.2) with a strength of 79.30 MPa.
 - e. The maximum tensile strength among the HSLWSCC mixes was obtained in Mix M8 (50% scoria and w/c = 0.2) with a strength of 5.38 MPa.
 - f. Mass loss was high at higher temperatures.
 - g. HSLWSCC mixes are more susceptible to fire in terms of spalling.
 - h. Developed NSLWSCC mixes are resistant to high temperatures and experience only minor cracks and holes even at 900°C.

Acknowledgments

The authors would like to acknowledge the support of the Australian Research Council Discovery Project (Grant No. DP180104035). The authors would like to express their sincere gratitude and appreciation to BASF and Abrams Marketing. The authors would also like to acknowledge Norbu Sonam for his assistance in carrying out the experimental work.

References

- Abdelaziz, G. E. 2010. "A study on the performance of lightweight self-consolidated concrete." *Mag. Concr. Res.* 62 (1): 39–49. <https://doi.org/10.1680/macr.2008.62.1.39>.

- Abouhussien, A. A., A. A. A. Hassan, and M. K. Ismail. 2015. "Properties of semi-lightweight self-consolidating concrete containing lightweight slag aggregate." *Constr. Build. Mater.* 75: 63–73. <https://doi.org/10.1016/j.conbuildmat.2014.10.028>.
- Andiç-Çakır, Ö., E. Yoğurtcu, Ş. Yazıcı, and K. Ramyar. 2009. "Self-compacting lightweight aggregate concrete: Design and experimental study." *Mag. Concr. Res.* 61 (7): 519–527. <https://doi.org/10.1680/macr.2008.00024>.
- Arioz, O. 2007. "Effects of elevated temperatures on properties of concrete." *Fire Saf. J.* 42 (8): 516–522. <https://doi.org/10.1016/j.firesaf.2007.01.003>.
- Aslani, F. 2013a. "Effects of specimen size and shape on compressive and tensile strengths of self-compacting concrete with or without fibers." *Mag. Concr. Res.* 65 (15): 914–929. <https://doi.org/10.1680/macr.13.00016>.
- Aslani, F. 2013b. "Pre-stressed concrete thermal behaviour." *Mag. Concr. Res.* 65 (3): 158–171. <https://doi.org/10.1680/macr.12.00037>.
- Aslani, F. 2014. "Experimental and numerical study of time-dependent behaviour of reinforced self-compacting concrete slabs." Ph.D. thesis, Dept. of Civil and Environmental Engineering, Univ. of Technology.
- Aslani, F. 2015a. "Creep behaviour of normal- and high-strength self-compacting concrete." *Struct. Eng. Mech.* 53 (5): 921–938. <https://doi.org/10.12989/sem.2015.53.5.921>.
- Aslani, F. 2015b. "Nanoparticles in self-compacting concrete—A review." *Mag. Concr. Res.* 67 (20): 1084–1100. <https://doi.org/10.1680/macr.14.00381>.
- Aslani, F. 2018. "Residual bond between concrete and reinforcing GFRP rebars at elevated temperatures." *Proc. Inst. Civ. Eng. Struct. Build.* 1–14. <https://doi.org/10.1680/jstbu.17.00126>.
- Aslani, F., and M. Bastami. 2011. "Constitutive models and relationships for normal and high strength concrete at elevated temperatures." *ACI Mater. J.* 108 (4): 355–364.
- Aslani, F., and M. Bastami. 2014. "Relationship between deflection and crack mouth opening displacement of self-compacting concrete beams with and without fibres." *Mech. Adv. Mater. Struct.* 22 (11): 956–967. <https://doi.org/10.1080/15376494.2014.906689>.
- Aslani, F., and J. Kelin. 2018. "Assessment and development of high-performance fibre-reinforced lightweight self-compacting concrete including recycled crumb rubber aggregates exposed to elevated temperatures." *J. Cleaner Prod.* 200 (1): 1009–1025. <https://doi.org/10.1016/j.jclepro.2018.07.323>.
- Aslani, F., G. Ma, and G. Muselin. 2018a. "Development of high-performance self-compacting concrete using waste recycled concrete aggregates and rubber granules." *J. Cleaner Prod.* 182: 553–566. <https://doi.org/10.1016/j.jclepro.2018.02.074>.
- Aslani, F., G. Ma, D. L. Y. Wan, and V. Le. 2018b. "Experimental investigation into rubber granules and their effects on the fresh and hardened properties of self-compacting concrete." *J. Cleaner Prod.* 172 (20): 1835–1847. <https://doi.org/10.1016/j.jclepro.2017.12.003>.
- Aslani, F., and L. Maia. 2013. "Creep and shrinkage of high strength self-compacting concrete: Experimental and numerical analysis." *Mag. Concr. Res.* 65 (17): 1044–1058. <https://doi.org/10.1680/macr.13.00048>.
- Aslani, F., L. Maia, and J. Santos. 2017. "Effect of specimen geometry and specimen preparation on the concrete compressive strength test." *Struct. Eng. Mech.* 62 (1): 97–106. <https://doi.org/10.12989/sem.2017.62.1.097>.
- Aslani, F., and M. Natoori. 2013. "Stress-strain relationships for steel fibre reinforced self-compacting concrete." *Struct. Eng. Mech.* 46 (2): 295–322. <https://doi.org/10.12989/sem.2013.46.2.295>.
- Aslani, F., and B. Samali. 2013. "Predicting the bond between concrete and reinforcing steel at elevated temperatures." *Struct. Eng. Mech.* 48 (5): 643–660. <https://doi.org/10.12989/sem.2013.48.5.643>.
- Aslani, F., and B. Samali. 2014a. "Constitutive relationships for steel fiber reinforced concrete at elevated temperatures." *Fire Technol.* 50 (5): 1249–1268. <https://doi.org/10.1007/s10694-012-0322-5>.
- Aslani, F., and B. Samali. 2014b. "Flexural toughness characteristics of self-compacting concrete incorporating steel and polypropylene fibers." *Aust. J. Struct. Eng.* 15 (3): 269–286. <https://doi.org/10.7158/S13-011.2014.15.3>.
- Aslani, F., and B. Samali. 2015. "Constitutive relationships for self-compacting concrete at elevated temperatures." *Mater. Struct.* 48 (1–2): 337–356. <https://doi.org/10.1617/s11527-013-0187-1>.
- AS (Standards Australia). 1974. *Methods for sampling and testing aggregates*. AS 1141-1974. Sydney, Australia: Standards Australia.
- AS (Standards Australia). 1991. *Method for securing and testing cores from hardened concrete for compressive strength*. AS 1012.14. Sydney, Australia: Standards Australia.
- AS (Standards Australia). 1994. *Supplementary cementitious materials for use with portland cement—Silica fume*. AS 3582.3. Sydney, Australia: Standards Australia.
- AS (Standards Australia). 1997. *Methods of testing concrete—Determination of the static chord modulus of elasticity and Poisson's ratio of concrete specimens*. AS 1012.17. Sydney, Australia: Standards Australia.
- AS (Standards Australia). 1998. *Aggregates and rock for engineering purposes. Part 1: Concrete aggregates*. AS 2758.1. Sydney, Australia: Standards Australia.
- AS (Standards Australia). 2000. *Chemical admixtures for concrete, mortar and grout—Admixtures for concrete*. AS 1478.1. Sydney, Australia: Standards Australia.
- AS (Standards Australia). 2001. *Supplementary cementitious materials for use with portland and blended cement—Slag—Ground granulated iron blast-furnace*. AS 3582. Sydney, Australia: Standards Australia.
- AS (Standards Australia). 2006. *Methods of testing portland and blended cements*. AS 2350. Sydney, Australia: Standards Australia.
- AS (Standards Australia). 2010a. *General purpose and blended cements*. AS 3972. Sydney, Australia: Standards Australia.
- AS (Standards Australia). 2010b. *Methods of testing concrete—Determination of indirect tensile strength of concrete cylinders ('Brazil' or splitting test)*. AS 1012.10. Sydney, Australia: Standards Australia.
- AS (Standards Australia). 2014. *Methods of testing concrete—Compressive strength tests—Concrete, mortar and grout specimens*. AS 1012.9. Sydney, Australia: Standards Australia.
- AS (Standards Australia). 2015. *Methods of testing concrete—Determination of properties related to the consistency of concrete—Slump flow, T500 and J-Ring test*. AS 1012.3.5. Sydney, Australia: Standards Australia.
- AS (Standards Australia). 2016. *Methods of test for supplementary cementitious materials for use with portland and blended cement*. AS 3583. Sydney, Australia: Standards Australia.
- ASTM. 2005. *Standard specification for silica fume used in cementitious mixtures*. ASTM C1240. West Conshohocken, PA: ASTM.
- Bastami, M., M. Baghbadrani, and F. Aslani. 2014. "Performance of nano-Silica modified high strength concrete at elevated temperatures." *Constr. Build. Mater.* 68: 402–408. <https://doi.org/10.1016/j.conbuildmat.2014.06.026>.
- Bingol, A. F., and R. Gul. 2004. "Compressive strength of lightweight aggregate concrete exposed to high temperatures." *Indian J. Eng. Mater.* 11: 68–72.
- Bogas, J. A., A. Gomes, and M. F. C. Pereira. 2012. "Self-compacting lightweight concrete produced with expanded clay aggregate." *Constr. Build. Mater.* 35: 1013–1022. <https://doi.org/10.1016/j.conbuildmat.2012.04.111>.
- Bozkurt, N. 2014. "The high temperature effect on fibre reinforced self-compacting lightweight concrete designed with single and hybrid fibers." *Acta Phys. Polonica A* 125 (2): 579–583. <https://doi.org/10.12693/APhysPolA.125.579>.
- Choi, Y. W., Y. J. Kim, H. C. Shin, and H. Y. Moon. 2006. "An experimental research on the fluidity and mechanical properties of high-strength lightweight self-compacting concrete." *Cem. Concr. Res.* 36 (9): 1595–1602. <https://doi.org/10.1016/j.cemconres.2004.11.003>.
- De Schutter, G., P. J. M. Bartos, P. Domone, and J. Gibbs. 2008. *Self-compacting concrete*. Scotland, UK: Whittles Publishing.
- EFNARC (European Federation of Specialist Construction Chemicals and Concrete Systems). 2002. "Specification and guidelines for self-compacting concrete." Accessed August 1, 2017. <http://www.efnarc.org/pdf/SandGforSCC.PDF>.
- EFNARC (European Federation of Specialist Construction Chemicals and Concrete Systems). 2005. "ERMCO the European guidelines for self-compacting concrete." Accessed August 1, 2017. www.efnarc.org/pdf/SCCGuidelinesMay2005.pdf.

- Fares, H., H. Toutanji, K. Pierce, and A. Noumowé. 2015. "Lightweight self-consolidating concrete exposed to elevated temperatures." *J. Mater. Civ. Eng.* 27 (12): 04015039. [https://doi.org/10.1061/\(ASCE\)MT.1943-5533.0001285](https://doi.org/10.1061/(ASCE)MT.1943-5533.0001285).
- Gai-Fei, P., and H. Zhi-Shan. 2008. "Change in microstructure of hardened cement paste subjected to elevated temperatures." *Constr. Build. Mater.* 22 (4): 593–599. <https://doi.org/10.1016/j.conbuildmat.2006.11.002>.
- Gencel, O. 2011. "Effect of elevated temperatures on mechanical properties of high-strength concrete containing varying proportions of hematite." *Fire Mater.* 36 (3): 217–230. <https://doi.org/10.1002/fam.1102>.
- Gesoglu, M., E. Güneyisi, T. Özturan, H. O. Oz, and D. S. Asaad. 2015. "Shear thickening intensity of self-compacting concretes containing rounded lightweight aggregates." *Constr. Build. Mater.* 79: 40–47. <https://doi.org/10.1016/j.conbuildmat.2015.01.012>.
- Gesoglu, M., E. Güneyisi, T. Özturan, H.Ö. Öz, and D. S. Asaad. 2014. "Permeation characteristics of self-compacting concrete made with partially substitution of natural aggregates with rounded lightweight aggregates." *Constr. Build. Mater.* 59: 1–9. <https://doi.org/10.1016/j.conbuildmat.2014.02.031>.
- Hassan, A. A. A., M. K. Ismail, and J. Mayo. 2015. "Mechanical properties of self-consolidating concrete containing lightweight recycled aggregate in different mixture compositions." *J. Build. Eng.* 4: 113–126. <https://doi.org/10.1016/j.jobe.2015.09.005>.
- Her-Yung, W. 2009. "Durability of self-consolidating lightweight aggregate concrete using dredged silt." *Constr. Build. Mater.* 23 (6): 2127–2131. <https://doi.org/10.1016/j.conbuildmat.2008.12.012>.
- Husem, M. 2006. "The effects of high temperature on compressive and flexural strengths of ordinary and high-performance concrete." *Fire Saf. J.* 41 (2): 155–163. <https://doi.org/10.1016/j.firesaf.2005.12.002>.
- ISO. 1999. *Part 1, Elements of building construction: General requirements for fire resistance testing*. ISO 834. London: ISO.
- Khaliq, W., and V. Kodur. 2011. "Thermal and mechanical properties of fiber reinforced high performance self-consolidating concrete at elevated temperatures." *Cem. Concr. Res.* 41 (11): 1112–1122. <https://doi.org/10.1016/j.cemconres.2011.06.012>.
- Kim, Y. J., Y. W. Choi, and M. Lachemi. 2010. "Characteristics of self-consolidating concrete using two types of lightweight coarse aggregates." *Constr. Build. Mater.* 24 (1): 11–16. <https://doi.org/10.1016/j.conbuildmat.2009.08.004>.
- Kivrak, S., M. Tuncan, M. I. Onur, G. Arslan, and O. Arioiz. 2006. "An economic perspective of advantages of using lightweight concrete in construction." In Vol. 16 of *Proc., 31st Conf. on Our World in Concrete and Structures*, 17. Singapore: CI-Premier PTE.
- Kodur, V. 2014. "Properties of concrete at elevated temperatures." *ISRN Civ. Eng.* 2014: 1–15. <https://doi.org/10.1155/2014/468510>.
- Koksal, F., O. Gencel, W. Brostow, and H. E. Hagg Lobland. 2012. "Effect of high temperature on mechanical and physical properties of lightweight cement based refractory including expanded vermiculite." *Mater. Res. Innov.* 16 (1): 7–13. <https://doi.org/10.1179/1433075X11Y.0000000020>.
- Law Yim Wan, D., F. Aslani, and G. Ma. 2018. "Lightweight self-compacting concrete incorporating perlite, scoria, and polystyrene aggregates." *J. Mater. Civ. Eng.* 30 (8): 04018178. [https://doi.org/10.1061/\(ASCE\)MT.1943-5533.0002350](https://doi.org/10.1061/(ASCE)MT.1943-5533.0002350).
- Lo, T. Y., P. W. C. Tang, H. Z. Cui, and A. Nadeem. 2007. "Comparison of workability and mechanical properties of self-compacting lightweight concrete and normal self-compacting concrete." *Mater. Res. Innovation* 11 (1): 45–50. <https://doi.org/10.1179/143307507X196239>.
- Maia, L., and F. Aslani. 2016. "Modulus of elasticity of concretes produced with basaltic aggregate." *Comput. Concr.* 17 (1): 129–140. <https://doi.org/10.12989/cac.2016.17.1.129>.
- Okamura, H., K. Ozawa, and M. Ouchi. 2000. "Self-compacting concrete." *Struct. Concr.* 1 (1): 3–17. <https://doi.org/10.1680/stco.2000.1.1.3>.
- Poon, C. S., Z. H. Shui, and L. Lam. 2004. "Compressive behavior of fiber reinforced high-performance concrete subjected to elevated temperatures." *Cem. Concr. Res.* 34 (12): 2215–2222. <https://doi.org/10.1016/j.cemconres.2004.02.011>.
- Ranjbar, M. M., and S. Y. Mousavi. 2015. "Strength and durability assessment of self-compacted lightweight concrete containing expanded polystyrene." *Mater. Struct.* 48 (4): 1001–1011. <https://doi.org/10.1617/s11527-013-0210-6>.
- Ries, J. P., D. A. Crocker, and S. R. Sheetz. 2003. *Guide for structural lightweight-aggregate concrete reported by ACI committee 213*, 1–38. Farmington Hills, MI: ACI.
- Taylor, P. 2013. *Curing concrete*. 1st ed. Boca Raton, FL: CRC Press.
- Topçu, I. B., and T. Uygunoğlu. 2010. "Effect of aggregate type on properties of hardened self-consolidating lightweight concrete (SCLC)." *Constr. Build. Mater.* 24 (7): 1286–1295. <https://doi.org/10.1016/j.conbuildmat.2009.12.007>.
- Wenzhong, Z., L. Haiyan, and W. Ying. 2012. "Compressive behaviour of hybrid fiber-reinforced reactive powder concrete after high temperature." *Mater. Des.* 41: 403–409. <https://doi.org/10.1016/j.matdes.2012.05.026>.
- Wu, Z., X. Wu, J. Zheng, T. Ueda, and S. Yi. 2013. "An experimental study on the performance of self-compacting lightweight concrete exposed to elevated temperature." *Mag. Concr. Res.* 65 (13): 780–786. <https://doi.org/10.1680/macr.12.00218>.
- Wu, Z., Y. Zhang, J. Zheng, and Y. Ding. 2009. "An experimental study on the workability of self-compacting lightweight concrete." *Constr. Build. Mater.* 23 (5): 2087–2092. <https://doi.org/10.1016/j.conbuildmat.2008.08.023>.
- Yehia, S., M. Alhamaydeh, and S. Farrag. 2014. "High-strength lightweight SCC matrix with partial normal-weight coarse-aggregate replacement: Strength and durability evaluations." *J. Mater. Civ. Eng.* 26 (11): 04014086. [https://doi.org/10.1061/\(ASCE\)MT.1943-5533.0000990](https://doi.org/10.1061/(ASCE)MT.1943-5533.0000990).